Nigerian Research Journal of Engineering and Environmental Sciences 6(1) 2021 pp. 1-11

Nigerian Research Journal of Engineering and Environmental Sciences
Journal homepage: www.rjees.com

Original Research Article

Pipe Grounding Conditions for AC Potential Reduction: An Extended Study

***Adedeji, K.B. and Ponnle, A.A.**

Department of Electrical and Electronics Engineering, School of Engineering and Engineering Technology, Federal University of Technology, PMB 704, Akure, Ondo State, Nigeria.
*kbadedeji@futa.edu.ng

ARTICLE INFORMATION

Article history:
Received 31 Dec, 2020
Revised 09 Apr, 2021
Accepted 22 Apr, 2021
Available online 30 Jun, 2021

Keywords:
AC interference
Induced potential
Pipelines
Pipe grounding
AC power lines

ABSTRACT

One of the strategies to reduce the influence of AC power line interference on pipelines is to ground the pipe at its end(s) or some points along the parallel route with the line. These strategies are referred to as grounding conditions and prior works in the literature have analyzed a number of these conditions for metal pipelines. However, in this study, it was discovered that the length of the parallel route can have an impact on the effectiveness of the grounding conditions. Thus, this effect was investigated using a real-life AC power line to pipeline interference problem. Additionally, for each grounding conditions, not only was the impact of the length of the parallel route examined but also the effectiveness of four dissimilar/different pipe coatings investigated. The AC power line to pipeline interference problem was formulated utilizing the notion of mutual impedance between two circuits. For each of the grounding conditions, it was discovered that the induced potential on the pipe varied substantially with variations in this length. Also, under these conditions, the effectiveness of some coatings in reducing the induced potential was discussed. In some of the coatings, AC potential of less than 50 V was observed on the pipe while in some cases, extremely high potential in the order of kV was observed depending on grounding condition and the exposed length considered.

1. INTRODUCTION

Globally, AC power line interference on pipelines is typically regarded as a major concern for pipeline owners. Amongst other issues, the problem is closely linked to the safety of operational personnel (Pham *et al*., 2003), the associated cost of corrosion (Qabazard and Elhirbawy, 2006) and pollution of the environment (Nassereddine *et al*., 2015; Grigsby, 2018; Ponnle and Adedeji, 2015). In situations where metal pipes are in parallel proximity to AC power lines, a considerable amount of voltage may be induced on the pipe amid steady state and fault conditions of the lines. In the event of fault occurrence on the line, potentials of extremely high magnitude may be induced on the pipe. Consequently, the induced potential may damage the materials of the pipe and is also dangerous to working personnel. An additional concern is the cost of maintaining and repairing the corroded pipes. The effect of the impressed potential in facilitating the corrosion process of pipes has been extensively investigated (Wen *et al.*, 2015; Guo *et al.*, 2017; Ouadah *et al.*, 2017a; 2017b; Wang *et al.*, 2018; Adedeji *et al.*, 2018).

Using electromagnetic field theory, when an AC line conductor is energized, a time-varying electromagnetic (EM) field (with electric E and magnetic H field components) is produced. The EM field causes voltage induction on the pipe in accordance with Equation (1).

$$e = \frac{\partial \varphi}{\partial t} \quad \varphi = \iint_s B \partial s \tag{1}$$

Where, e is the induced potential, φ and B denote the magnetic flux and flux density generated by the fields, while s represents the area of enclosed loop initiated by the field. Conventionally, for underground pipes, the E component of the field is considered insignificant. This is because of the screened effect of the ground towards E-fields. Therefore, a major concern for underground and above-ground pipes is the H component of the field. In view of this, countless studies were carried out to assess the impact of these fields on underground and above-ground pipes (Abdel-Gawad *et al.*, 2015; Ponnle *et al.*, 2015; 2017; Wu *et al.*, 2017; Lucca, 2019; Popoli *et al.*, 2019; 2020; Al-Gabalawy *et al.*, 2020). The most fascinating thing is that Ponnle *et al.* (2015) discovered the horizontal H-field part promotes the induction when considering underground pipes. Therefore, reducing the induced potential on the pipe is crucial for safety and safeguarding of pipe materials.

Years back, discussions were made about lessening the impact of AC potential on metal pipes with diverse AC mitigation methodologies proposed (Southey *et al.*, 1994; Tachick, 2001; Markovic *et al.*, 2005). Preliminary proposals to curtailing the impact of AC interference on metal pipes varied from the application of zinc ribbon, AC decoupling devices, ground control mats, special backfill, gradient control wires, and Faraday cage (Southey *et al.*, 1994; Tachick, 2001; Markovic *et al.*, 2005). Surprisingly, these methodologies have not been able to effectively mitigate AC interference (Gregoor *et al.*, 2001; Shwehdi and Al-qahtani, 2010). In some other research works (NACE, 2014; Adedeji, 2016; Adedeji *et al.*, 2017; MATCOR, 2019), it has been reported that the use of a lumped grounding system where metal pipes are grounded at its ends or points along the route with the power line will significantly minimize the level of the AC potential. Thus, among these mitigation systems, the lumped grounding system provides better protection to pipes during steady-state or fault conditions from nearby AC power lines (MATCOR, 2019). Therefore, a pipe can be grounded from a point x=0 to x=L along its length as shown in Figure 1.

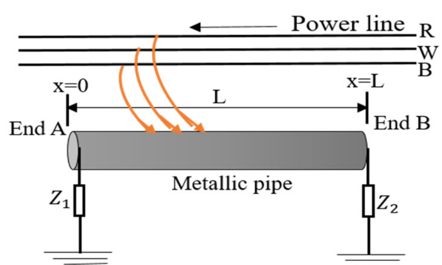

Figure 1: Lumped grounding for AC potential mitigation (Tleis, 2008)

Exploiting one or a hybrid of those systems will be an improved or alternative way to minimize the level of AC potentials on the pipe albeit with significant implementation cost. To this end, Adedeji *et al.* (2017),

K.B. Adedeji and A.A. Ponnle / Nigerian Research Journal of Engineering and Environmental Sciences
6(1) 2021 pp. 1-11

verified the several categories of the lumped grounding conditions to indicate the most effective ones in reducing AC potential level without taking the effect of the pipe exposed length into considerations. However, it is postulated in this work that when taking the pipe's exposed length into consideration, the effectiveness of the grounding conditions can be scrutinized. The pipe's exposed length in this context refers to the length of the parallel route with the power line. Thus, the influence of this key parameter on the grounding conditions is presented in this paper. Furthermore, the performance considering four dissimilar pipe coatings was evaluated. The coatings considered are bitumen (BT), polyurethane (PU), polyethylene (PE), and fusion bonded epoxy (FBE).

2. METHODOLOGY

2.1. AC Power Line-Pipeline Interference Model

In the problem formulation, the notion of mutual impedance between two circuits was adopted considering a balanced system (Ouadah, and Zergoug, 2014). Figure 2 shows the description of the power line-pipeline interference considered.

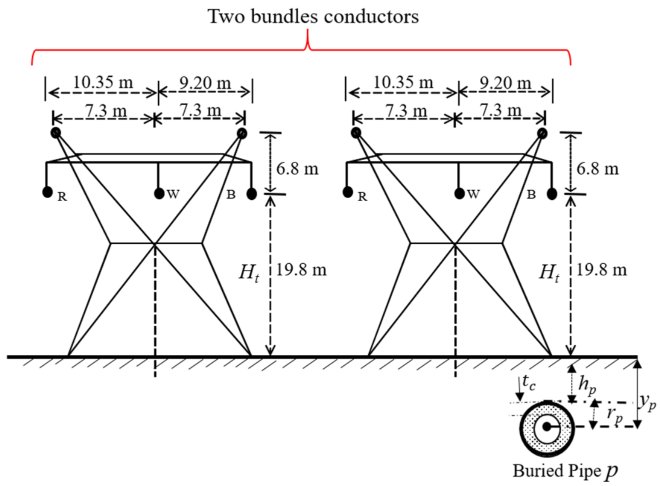

Figure 2: The studied power line-pipeline interference problem

As may be observed, the two lines are horizontal single-circuit lines with two bundle conductors. The pipe considered is an underground type with a burial depth of h_p which spans parallel to the power line. In the model formulation, the reciprocal effect of the earth wires on each other is considered insignificant. In the two power lines system shown in Figure 2, each of these lines produces an inductive coupling effect on the pipe. Therefore, the total induced potential (E_{pipe}) may be evaluated as:

$$E_{pipe} = \sum_{i} E_{T-i} \qquad i \in (1, \ldots.., N) \tag{2}$$

Where, $E_{T\text{-}i}$ denotes the induced potential due to the i^{th} power line and N is the total number of the power lines considered. If A, B, C represent the notation of the line's phase conductors, the induced potential on the pipe considering the effect of an i^{th} power line is given as:

$$E_{T-i} = I_{A-i}Z_{A-ip} + I_{B-i}Z_{B-ip} + I_{C-i}Z_{C-ip} - \sum_{k=1}^{n} I_{g_k-i}Z_{g_{k-i}p} \tag{3}$$

In Equation (3), I_{A-i}, I_{B-i}, I_{C-i} and I_{gk-i} represent the steady-state phase conductor currents and the earth wire currents, while mutual impedances (Ω/m) between these conductors, the earth wire and the pipe are represented by Z_{A-ip}, Z_{B-ip}, Z_{C-ip}, Z_{gk-ip}. The I_{A-i},, I_{B-i},, I_{C-i} alternates at a phase angle of 120°, 0°, -120°. Also, n is used to represent the number of earth wires. If the potential (E_{gk}) and current I_{gk} across the earth wire is estimated as:

$$E_{gk} = I_{R-i}Z_{R-igk} + I_{W-i}Z_{W-ig_k} + I_{B-i}Z_{B-ig_k}\,;\; I_{g_k} = \frac{1}{Z_{ggk-i}}\left(I_{R-i}Z_{R-ig_k} + I_{W-i}Z_{W-ig_k} + I_{B-i}Z_{B-ig_k}\right) \tag{4}$$

The potential on the pipe considering the effect of an i^{th} power line is given as:

$$\begin{aligned} E_{T-i} = {} & I_{A-i}\left(Z_{A-ip} - \sum_{k=1}^{n}\frac{Z_{A-ig_k}Z_{g_{k-i}p}}{Z_{gg_{k-i}}}\right) + I_{B-i}\left(Z_{B-ip} - \sum_{k=1}^{n}\frac{Z_{B-ig_k}Z_{g_{k-i}p}}{Z_{gg_{k-i}}}\right) \\ & + I_{C-i}\left(Z_{C-ip} - \sum_{i=1}^{n}\frac{Z_{C-ig_k}Z_{g_{k-i}p}}{Z_{gg_{k-i}}}\right) \end{aligned} \tag{5}$$

The k^{th} earth wire self-impedance Z_{ggk-i} of the i^{th} power line is expressed as:

$$Z_{gg_{k-i}} = {\pi f \mu_0}/{4} + R_{g_{k-I}} + j\left(f\mu_0\left\{\frac{1}{4} + \log_e\left(\frac{\Delta_e}{R_{GM_{k-i}}}\right)\right\}\right) \tag{6}$$

Where, f and μ_0 denote the power line frequency of operation and the free space permeability respectively. R_{gk-i} and R_{GMk-i} are the k^{th} earth wire AC resistance and its geometric mean radius. The mutual impedance linking two circuits (for instance τ and pipe p) is evaluated as:

$$Z_{\tau-i-p} = \frac{\pi f \mu_0}{4} + j\left(\left((f\mu_0)\log_e\left\{\frac{\Delta_e}{D_{\tau-i-p}}\right\}\right)\right), \tau - i \in \{A, B, C, g_k\} \tag{7}$$

In Equation (7), the geometric mean distance (GMD) associating $\tau - i \in \{A, B, C, g_k\}$ and the pipe is represented by $D_{\tau-i-p}$. From Equation (7) as well, the earth's skin depth Δ_e is determined using the earth relative permittivity (μ_r) and the soil resistivity (ρ) as:

$$\Delta_e = \sqrt{\frac{\rho}{\mu f}}, \mu = \mu_r \mu_0 \tag{8}$$

The relative permeability for soils ranges from 1.00001 to 1.14 (Scott, 1996). In Equation (7), it is also possible to estimate the GMD associating $\tau - i \in \{A, B, C, g_k\}$ and the pipe using Equation (9).

$$D_{\tau-i-p} = \left\{\left(x_p - x_{\tau-i}\right)^2 + \left(y_{\tau-i} - y_p\right)^2\right\}^{\frac{1}{2}}, \tau - i \in \{A, B, C, g_k\} \tag{9}$$

In Equation (9), x_p is used to represents the location of the pipe across the power line while y_p denotes the depth from ground to the centre of the pipe. Usually, in the estimation of y_p, the pipe radius r_p, pipe coating thickness t_c, and the h_p are used as $y_p=h_p+r_p+t_c$. Likewise, in Equation (9), $x_{\tau-i}$ denotes the horizontal location for $\tau - i \in \{A, B, C, g_k\}$ while $y_{\tau-i}$ is used to denote their vertical location.

The expressions in Equation (5) permits the appraisal of the longitudinal induced EMF (V/m) on a pipe parallel to a power line. Nonetheless, if a pipe is modelled as a lossy transmission line with series impedance Z_s, shunt admittance Y_{sh} and a potential source respectively, it is possible to estimate the induced potential (V) at points along the parallel route as illustrated in Figure 3. This potential is usually regarded as the pipe-to-soil potential.

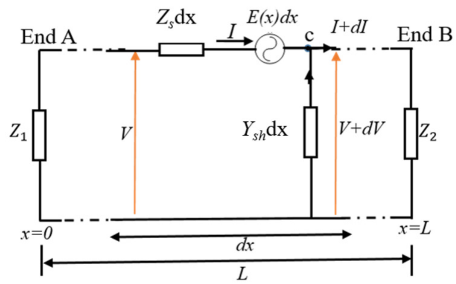

Figure 3: An equivalent circuit of power line-pipeline inductive coupling

By resolving the conventional power lines differential equations associating E, V, and I respectively, the potential through the pipe incremental length dx may be evaluated. Consequently, at a point x through the pipe, the induced potential (V) may be estimated using Equation (10) (Adedeji, 2016; Adedeji *et al.*, 2017).

$$V(x) = E_{pipe}/\gamma \left[\frac{\left\{ Z_2 e^{-\gamma x}(Z_1 - Z_0) - Z_1(Z_2 + Z_0)e^{\gamma(L-x)} \right\} - \left\{ Z_1 e^{-\gamma(L-x)}(Z_2 - Z_0) - Z_2(Z_1 + Z_0)e^{\gamma x} \right\}}{(Z_1 + Z_0)(Z_2 + Z_0)e^{\gamma L} - (Z_1 - Z_0)(Z_2 - Z_0)e^{-\gamma L}} \right] \quad (10)$$

In Equation (10), Z_1 and Z_2 are the impedances at x=0 and x=L while γ is the pipe propagation constant and L is the pipe exposed length along the parallel route. The characteristic impedance Z_0 of the pipe and its propagation constant is given as:

$$Z_0 = \left(Z_s / Y_{sh} \right)^{\frac{1}{2}} \quad \text{and} \quad \gamma = \left(Z_s Y_{sh} \right)^{\frac{1}{2}} \quad (11)$$

In Figure 3, the traditional expression for Z_s (Ω/m) and Y_{sh} (Ω^{-1}/m) considering a buried coated pipe (CIGRE, 1995) is given as:

$$\left. \begin{aligned} Z_s &= \frac{1}{2\pi r_p}\left(\pi f \rho_p \mu_0 \mu_p\right)^{\frac{1}{2}} + \frac{\pi f \mu_0}{4} + j\left[\frac{1}{2\pi r_p}\left(\pi f \rho_p \mu_0 \mu_p\right)^{\frac{1}{2}} + \mu_0 f \ln\left(\frac{3.7}{2r_p}\sqrt{\frac{\rho}{2\pi f \mu_0}} \right) \right] \\ Y_{sh} &= \frac{2\pi r_p}{\rho_c t_c} + j\left(2\pi f \left(\frac{2\varepsilon_0 \varepsilon_c \pi r_p}{t_c} \right) \right) \end{aligned} \right\} \quad (12)$$

In Equation (12), both μ_p and ρ_p denote the pipe material relative permeability and resistivity, ρ_c and ε_c are the coating resistivity and relative permittivity, while ε_0 represents the permittivity of free space. The equations described above allow the examination of the impact of the varying pipe exposed length on the level of the induced potential through the pipe considering the grounding conditions and pipe coatings. In this work, the following categories of the lumped pipe grounding conditions were considered (Adedeji, 2016; Adedeji *et al*., 2017):

(a) Category (i): When the pipe extends for some kilometres beyond points x=0 and x=L; thus $Z_1 \Rightarrow Z_2 \Rightarrow Z_0$.

(b) Category (ii): When the pipe is isolated at x=L with an insulating flange and continues at x=0; thus $Z_1 \Rightarrow Z_0; Z_2 \Rightarrow \infty$.

(c) Category (iii): The pipeline continues beyond x=L and grounded at x=0; thus $Z_1 \Rightarrow 0; Z_2 \Rightarrow Z_0$.

(d) Category (iv): The pipe is isolated at x=0 and x=L with an insulating flange; thus $Z_1 \Rightarrow Z_2 \Rightarrow \infty$.

The evaluations and analysis were conducted using MATLAB.

2.2. The AC Power Line-Pipeline Data

Table 1 and Table 2 illustrate the data relating to the power line-pipeline interference problem considered. Along the power line, the pipe is located 24 *m* away which is equivalent to Eskom's power line servitude for 275 *kV*–400 *kV* lines in South Africa (Eskom, 2015). Additionally, measurements conducted around the power line-pipeline site revealed that the neighbouring soil can be presumed to be homogeneous with a resistivity of 12.96 Ω*m*.

Table 1: The power line data

Parameter	Value
Operating voltage	275 *kV*
Maximum allowable current at 275 kV	410 *A* per conductor
Diameter of the earth wire	13.48 *mm*
Earth wire resistivity	45×10^{-8} Ω*m*
AC resistance of the earth wire	3.44×10^{-3} Ω/*m*

Table 2: The pipeline data.

Parameter	Value
Pipe radius	500 *mm*
Burial depth	1 *m*
Pipe coating resistance	4 *mm*
Resistivity of the neighbouring soil	12.96 Ω*m*

3. RESULTS AND DISCUSSION

Figure 4 illustrates the pipe-to-soil potential outline for the first category of the pipe grounding conditions considered for a varying pipe exposed length L from 0.5 *km* to 10 *km*. Also demonstrated is the impact of the coatings for each condition as stated in the previous sections. In Figure 5 the pipe-to-soil potential outline for the second category of the pipe grounding conditions considered for a varying pipe exposed length L from 0.5 *km* to 10 *km* is demonstrated. Figure 6 shows the pipe-to-soil potential outline for conditions (iii) considered for a varying pipe exposed length L from 0.5 k*m* to 10 *km* is demonstrated while Figure 7 illustrates the pipe-to-soil potential outline for the fourth category of the pipe grounding conditions considered.

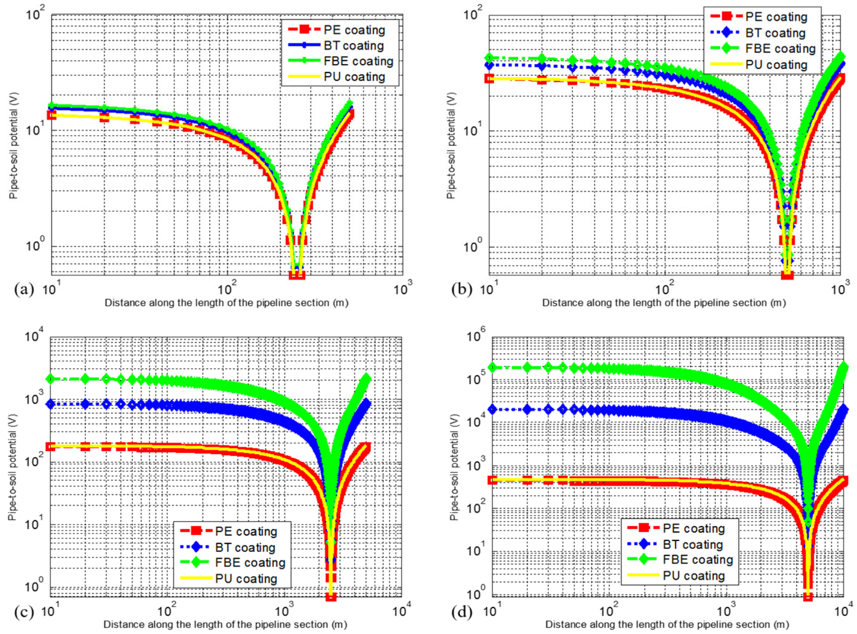

Figure 4: Profile of pipe-soil-potential for grounding category (i): (a) *L*=0.5 *km* (b) *L*=1 *km* (c) *L*=5 *km* (d) *L*=10 *km*

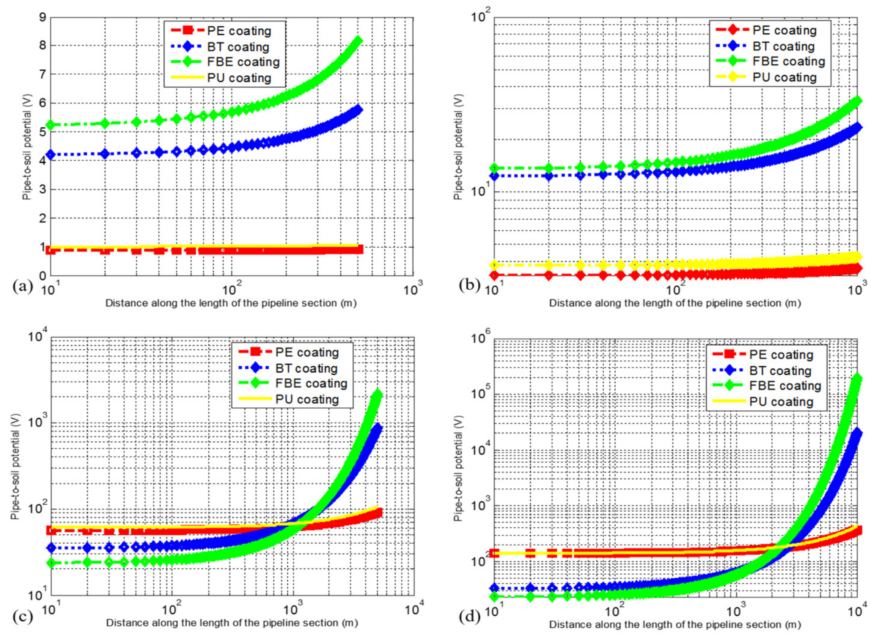

Figure 5: Profile of pipe-soil-potential for grounding category (ii): (a) *L*=0.5 *km* (b) *L*=1 *km* (c) *L*=5 *km* (d) *L*=10 *km*

K.B. Adedeji and A.A. Ponnle / Nigerian Research Journal of Engineering and Environmental Sciences
6(1) 2021 pp. 1-11

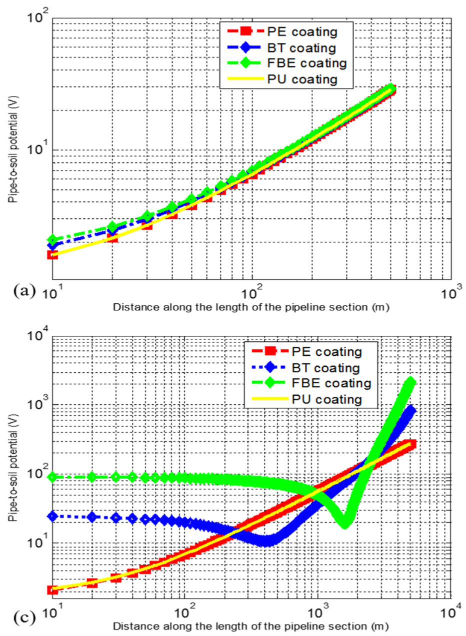

Figure 6: Profile of pipe-soil-potential for grounding category (iii): (a) L=0.5 *km* (b) L=1 *km* (c) L=5 *km* (d) L=10 *km*

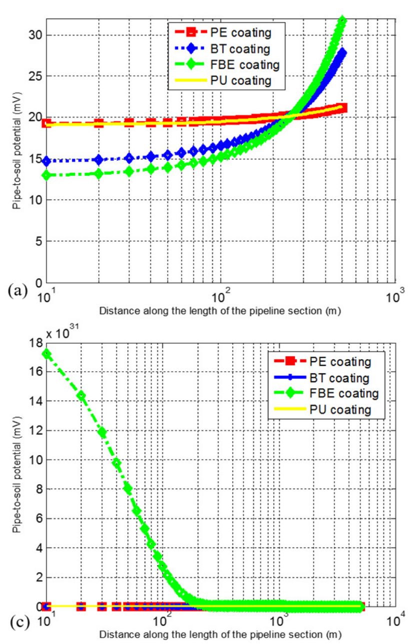

Figure 7: Profile of pipe-soil-potential for grounding category (iv): (a) L=0.5 *km* (b) L=1 *km* (c) L=5 *km* (d) L=10 *km*

In Figure 4, it was discovered that increasing the exposed length increases the induced potential level. Moreover, when the impact of the coatings on this grounding category is considered, an important information is observed. For this grounding category, some of the coatings perform an excellent job on the potential level. At first, the response of all the coatings considered is quite similar, that is, the potential increases for all the coatings with no remarkable changes spotted for lower exposed lengths. However, with higher exposed length, a remarkable change in potential level among the coatings is noticed as may be observed in Figure 4(c) and Figure 4(d). This confirms that the performance of the PE and PU coatings is better than those of BT and FBE coatings under this condition. This is one of the reasons why a good coating type is important when selecting a pipe grounding category for minimizing the potential level.

Considering Figure 5, a relatively low induced potential level is noticed for values of *L* in contrast to the grounding category (i). As far as the coating is concerned, only PE and PU coatings are observed to produce good results for lower values of *L* such as 0.5 and 1 *km*. Notwithstanding, when higher values of *L* such as 5 and 10 *km* are considered, the shape of the induced potential level for the four coatings considered is quite similar as may be noticed in Figure 5(c) and Figure 5(d). In this case, the performance of both FBE and BT coatings is okay up to about 1000 *m* along the pipe length. A distance above this indicates good performance of both PU and PE coatings with lower values of induced potential.

Considering the results for the grounding category (iii) as illustrated in Figure 6, it is discovered that increasing the exposed length raises the induced potential level. For certain values of *L*, the potential level for grounding category (iii) is comparatively lower than those in category (i). As far as the coating is concerned, the potential level along the pipe length is nearly the same for the four coatings when considering value of $L \geq 1$ *km*. Above this, the performance of both PU and PE coatings is good for distances up to about 300 *m* as shown in Figure 6(c). Notwithstanding, when distances from 300 *m* to 1000 *m* along the pipe length was considered, only BT coating was observed to provide a reduced level of the induced potential. Above these, FBE coating has a superior performance. Considering Figure 6(d), it may be observed that both the PU and PE coatings have superior performance throughout the distance along the pipe length.

In Figure 7 which illustrates the pipe-to-soil potential outline for the grounding conditions (iv), and in contrast to the results presented in Figure 6 (a) and Figure 6(b) for grounding category (iii), a comparatively low AC potential level (between 10 to 50 *V*) is noticed for 0.5 *km* and 1 *km* values of the exposed length. Considering the coating performance, both FBE and BT coatings give a reduced level of AC potential (between 8 *V* to about 17 *V*) up to some distances along the length of the pipe. Nevertheless, at values of *L* above 1 *km*, extremely high AC potential (in the order of *kV*) is noticed on the pipe as may be seen in Figure 7(c) and Figure 7(d). Also, in Figure 7(d), the profile of the induced potential level for the four coatings is quite similar. As may be noticed in both Figure 7(c) and Figure 7(d), the simulation results revealed that FBE coating (Figure 7(c)) and BT coating (Figure 7(d)) gives extremely high induced potentials at some distances along the pipe (in the order of *kV*) for grounding category (iv). Therefore, both FBE and BT coatings should not be used on a pipe with grounding category (iv) for values of *L* above 1 *km*. It is important to mention that the results presented is in tandem with those presented by Chen *et al.* (2018) which indicates that the induced potential on the pipe increases with the pipe exposure length for AC rail lines. In the current study, investigations on the impact of this parameter on the pipe grounding conditions and coatings was further analyzed and discussed in this paper.

4. CONCLUSION

Installing pipelines in the same route with power lines is increasingly common howbeit with the associated problem of AC interference. Nonetheless, a feasible approach to minimizing the level of the induced potential is to ground the pipe at its end(s) or some points along the parallel route with the line. However, in this study, it was discovered that taking the exposed length of the pipe into consideration has an impact on the way in which the pipe can be grounded. Thus, this effect was investigated using a real-life AC power line to pipeline interference problem. In addition to this, the effectiveness of four dissimilar pipe coatings under this effect was discussed. The results presented revealed the significance of the exposed length and the coating types when considering pipe grounding methodologies for AC potential reduction. The AC potential on the pipe varies substantially with variations in the exposed length for the grounding categories considered. Also, under these conditions, the effectiveness of some coatings in minimizing the AC potential level is better. The results also revealed that for exposed length above 1 *km*, lumped grounding category (iv) should not be applied.

5. CONFLICT OF INTEREST

There is no conflict of interest associated with this work.

REFERENCES

Abdel-Gawad, N.M., El Dein, A.Z. and Magdy, M. (2015). Mitigation of induced voltages and AC corrosion effects on buried gas pipeline near to OHTL under normal and fault conditions. *Electric Power Systems Research*, 127, pp. 297–306.

Adedeji, K.B. (2016). Development of an assessment model and graphical user interface for monitoring alternating current interference induced corrosion of buried pipelines. M.Tech. Dissertation, Department of Electrical Engineering, Tshwane University of Technology, Pretoria, South Africa.

Adedeji, K.B., Abe, B.T., Hamam, Y., Abu-Mahfouz, A.M., Shabangu, T.H. and Jimoh, A.A. (2017). Pipeline grounding condition: A control of pipe-to-soil potential for ac interference induced corrosion reduction. In: Proceedings of the 25th SAUPEC Conference, January 30 to February 1st, Stellenbosch, South Africa.

Adedeji, K.B., Ponnle, A.A., Abe, B.T., Jimoh, A.A., Abu-Mahfouz, A.A. and Hamam Y. (2018). AC induced corrosion assessment of buried pipelines near HVTLs: A case study of South Africa. *Progress in Electromagnetics Research B*, 81, pp. 45–61.

Al-Gabalawy, M., Mostafa, M.A., Hamza, A.S. and Hussein, S.A. (2020). Modelling of the KOH^- polarization cells for mitigating the induced AC voltage in metallic pipelines. *Heliyon*, 6(3), p. e03417.

CIGRE. (1995). Guide on the influence of high voltage AC power systems on metallic pipelines. In: CIGRE Working Group 36.02 Technical Brochure No. 095.

Chen, M., Liu, S., Zhu, J., Xie, C., Tian, H and Li, J. (2018). Effect and characteristics of AC interference on parallel underground pipelines caused by an AC electrified railway. *Energies*, 11, pp. 1-24.

Eskom. (2015). Guideline on the electrical coordination of pipelines and power lines. Revision 1, Section 3.1.3.2, 13.

Gregoor, R., Pourbaix, A. and Carnentiers, P. (2001). Detection of AC corrosion. In: CEOCOR Congress, October 2-5, Biarritz, France, Paper No. 2, pp. 1–14.

Grigsby, L.L. (2018). *Electric Power Generation, Transmission, and Distribution*. 3rd ed., CRC press, Boca Raton, Florida, USA.

Guo, Y., Meng, T., Wang, D., Tan, H. and He, R. (2017). Experimental research on the corrosion of X series pipeline steels under alternating current interference. *Engineering Failure Analysis*, 78, pp. 87–98.

Lucca, G. (2019). AC Interference from a faulty power line on nearby buried pipeline: Influence of the surface layer soil. *IET Science, Measurement and Technology*, 14, pp. 225-232.

Markovic, D., Smith, V. and Perera, V. (2005). Evaluation of gradient control wire and insulating joints as methods of mitigating induced voltages in gas pipelines. In: Proceedings of the AUPEC Conference, September 25-28, Hobart, Australia.

MATCOR (2019). AC mitigation: 4 approaches. MATCOR Inc. Available: https://www.matcor.com/ac-mitigation/. [Accessed: 22 April 2019].

NACE SP0177-2014. Mitigation of alternating current and lightning effects on metallic structures and corrosion control systems. NACE International, Houston, Texas, 2014.

Nassereddine, M., Rizk, J., Hellany, A. and Nagrial, M. (2015). Induced voltage behaviour on pipelines due to HV AC interference under broken OHEW. In: IEEE 10th Conference on Industrial Electronics and Applications, June 15-17, Auckland, New Zealand, 1408-1413.

Ouadah, M. H. and Zergoug, M. (2014). Analysis of the electromagnetic interferences between overhead power lines and buried pipelines. *Mediterranean Journal of Modelling and Simulation,* 1, pp. 13-23.

Ouadah, M., Touhami, O., Ibtiouen, R., Benlamnouar, M.F. and Zergoug, M. (2017a). Corrosive effects of the electromagnetic induction caused by the high voltage power lines on buried X70 steel pipelines. *International Journal of Electrical Power & Energy Systems*, 91, pp. 34–41.

Ouadah, M.H., Touhami, O., Ibtiouen, R. and Zergoug, M. (2017b). Method for diagnosis of the effect of AC on the X70 pipeline due to an inductive coupling caused by HVPL. *IET Science, Measurement & Technology*, 11, pp. 766–772.

Pham, K.D., Thomas, R.S. and Stinger, W.E. (2003). Operational and safety considerations for light rail DC traction electrification system design. In: 9th National Light Rail Transit Conference, November 16–18, Portland, Oregon, USA.

Ponnle, A. and Adedeji, K. (2015). Assessment of human exposure to magnetic field from overhead high voltage transmission lines in a city in south western Nigeria. *American Journal of Engineering Research*, 4, pp. 154–162.

Ponnle, A.A., Adedeji, K.B., Abe, B.T. and Jimoh, A.A. (2015). Planar magnetic field distribution underneath two-circuit linear configured power lines in various phase arrangement. In: Proceedings of the 12th IEEE AFRICON Conference, September 14-17, Ethiopia, pp. 777–781.

Ponnle, A.A., Adedeji, K.B., Abe, B.T. and Jimoh, A.A. (2017). Variation in phase shift of phase arrangements on magnetic field underneath overhead double-circuit HVTLs: Field distribution and polarization study. *Progress in Electromagnetics Research M*, 56, pp. 157–167.

Popoli, A., Sandrolini, L. and Cristofolini, A. (2019). A quasi-3D approach for the assessment of induced AC interference on buried metallic pipes. *International Journal of Electrical Power and Energy System*, 106, pp. 538-545.

Popoli, A., Sandrolini, L. and Cristofolini, A. (2020). Inductive coupling of metallic pipeline: Effect of a non-uniform soil resistivity along a pipeline-power line corridor. *Electric Power System Research*, 189, p. 106621.

Qabazard, A.M. and Elhirbawy, M.A. (2006). Corrosion and electromagnetic field coupling in the state of Kuwait. In: IEEE 11th International Conference on Transmission & Distribution Construction, Operation and Live-Line Maintenance, October 15–19, Albuquerque, USA.

Scott, J.H. (1996). Electrical and magnetic properties of rock and soil. US Geological Survey Technical Letter, Special Projects-16.

Shwehdi, M. and Al-qahtani, B. (2010). Cost-effective mitigation study of electromagnetic interference by power lines on neighbouring gas pipeline. In: CIGRE Colloquium on Lightning and Power System, May 16-19, Kuala Lumpur, Malaysia.

Southey, R., Dawalibi, F. and Vukonich, W. (1994). Recent advances in the mitigation of AC voltages occurring in pipelines located close to electric transmission lines. *IEEE Transactions on Power Delivery*, 9, pp. 1090–1097.

Tachick, H. (2001). AC mitigation using shield wires and solid-state decoupling devices. *Materials Performance*, 40, pp. 24–27.

Tleis, A. D. N. (2008). *Power Systems Modelling and Fault Analysis: Theory and Practice.* Newnes Press, Oxford, UK.

Wang, L., Cheng, L., Li, J., Zhu, Z., Bai, S. and Cui, Z. (2018). Combined effect of alternating current interference and cathodic protection on pitting corrosion and stress corrosion cracking behaviour of X70 pipeline steel in near-neutral pH environment. *Materials*, 11(4), pp. 1–19.

Wen, C., Li, J., Wang, S. and Yang, Y. (2015). Experimental study on stray current corrosion of coated pipeline steel. *Journal of Natural Gas Science and Engineering*, 27, pp. 1555–1561.

Wu, X., Zhang, H. and Karady, G.G. (2017). Transient analysis of inductive induced voltage between power line and nearby pipeline. *International Journal of Electrical Power & Energy Systems*, 84, pp. 47–54.